

# **Central Lancashire Online Knowledge (CLoK)**

Title	Development and validation of a model for transient lubricant transport following start-up in a spray lubricated, motored marine diesel engine simulator
Type	Article
URL	https://clok.uclan.ac.uk/id/eprint/57033/
DOI	https://doi.org/10.1016/j.triboint.2025.111266
Date	2026
Citation	Calderbank, Graham John, Sherrington, Ian and Smith, Edward H (2026) Development and validation of a model for transient lubricant transport following start-up in a spray lubricated, motored marine diesel engine simulator. Tribology International, 214 (Part B). p. 111266. ISSN 0301-679X
Creators	Calderbank, Graham John, Sherrington, Ian and Smith, Edward H

It is advisable to refer to the publisher's version if you intend to cite from the work. https://doi.org/10.1016/j.triboint.2025.111266

For information about Research at UCLan please go to <a href="http://www.uclan.ac.uk/research/">http://www.uclan.ac.uk/research/</a>

All outputs in CLoK are protected by Intellectual Property Rights law, including Copyright law. Copyright, IPR and Moral Rights for the works on this site are retained by the individual authors and/or other copyright owners. Terms and conditions for use of this material are defined in the <a href="http://clok.uclan.ac.uk/policies/">http://clok.uclan.ac.uk/policies/</a>

ELSEVIER

Contents lists available at ScienceDirect

## Tribology International

journal homepage: www.elsevier.com/locate/triboint



## Development and validation of a model for transient lubricant transport following start-up in a spray lubricated, motored marine diesel engine simulator

G. Calderbank\*, I. Sherrington, E.H. Smith

Jost Institute for Tribotechnology, School of Engineering and Computing, University of Lancashire, Preston PR1 2HE, UK

#### ARTICLE INFO

#### Keywords:

Large two-stroke marine engine Lubricant transport Oil film thickness measurement Lubrication modelling

#### ABSTRACT

This paper presents a model of the development of lubricating film thickness and film extent in a cross-head engine operated from start-up under motoring, along with experimental validation using an engine simulator. Theoretical predictions and experimental measurements of oil film thickness, and axial and radial ring gap filling under lubricant transport are presented with crank angle resolution on an instantaneous basis over several engine strokes following start-up. The experimental equipment and simulation model permit delivery of lubricant in a range of quantities (volumes of 0.01 mL and 0.04 mL per injector are discussed here). The delivery interval (every stroke, every second stroke, etc), number of injectors used and timing of injection (measured from the top of the stroke) can also be varied in the test equipment although they remained constant (injecting once per cycle at bottom dead-centre) for the work presented here. The novel, multi-stroke theoretical model simulates operation of the test equipment. On system start-up, it was found that axial distribution of the lubricant under Couette flow occurred more quickly than circumferential distribution under Poiseuille flow. It was also shown that lubricant distribution occurs in several distinct steps which the authors have linked to physical stages of the filling process. The aim of the study was to gain a quantitative understanding of the lubricant distribution mechanism, with the long-term aim of supporting steps to minimise the lubricant delivery rates for large, twostroke marine engines, and thus reduce operating costs and engine emissions due to the combustion of lubricating oil.

## 1. Introduction

For a given mass of freight, using large container ships at sea to transport freight has been demonstrated to be as much as two orders of magnitude less polluting than transport by other means such as road and air [1]. However, it has been estimated that around 70 % of ship emissions are released within 400 km of land. Due to the scale of the shipping industry, this has led to air degradation in coastal areas involving shipping related emissions contributing significant levels of particulate matter in ambient air (1–7 % of PM10, 1–14 % of PM2.5, and at least 11 % of PM1) in Europe [2]. Shipping also contributes to up to 24 % of NO<sub>2</sub> levels, with the highest levels in the Netherlands and Denmark [3]. Most of these emissions are due to fuel combustion, but they are also partly due to combustion of lubricants.

In large two-stroke marine diesel engines, the cylinder is separated from the rest of the engine for two reasons. Firstly, these engines run on lower-quality bunker fuels which often contain contaminants which may be abrasive. Secondly, the historic high sulphur content of these fuels has led to the development of acidic combustion products in the lubricating oil which cause corrosion. In some situations, this can be at its most aggressive when the engine is not operating, in a process called "cold corrosion" [4].

The lubrication arrangement for these engines incorporates a crosshead bearing and a stuffing box, as shown in Fig. 1. This arrangement significantly reduces the transfer of abrasive and corrosive materials to the rest of the engine, thus reducing corrosion and wear in locations in the engine away from the cylinder. However, it also requires that lubricant is supplied separately to the cylinder to lubricate the ring-pack and piston skirt. Cylinder lubricant is mostly burnt and ejected from the engine with other gaseous products of combustion. (Although some lubricant moves to the bottom of the cylinder). This approach to lubrication is almost a total loss system, so it is beneficial to minimise the

E-mail address: gjcalderbank@lancashire.ac.uk (G. Calderbank).

<sup>\*</sup> Corresponding author.

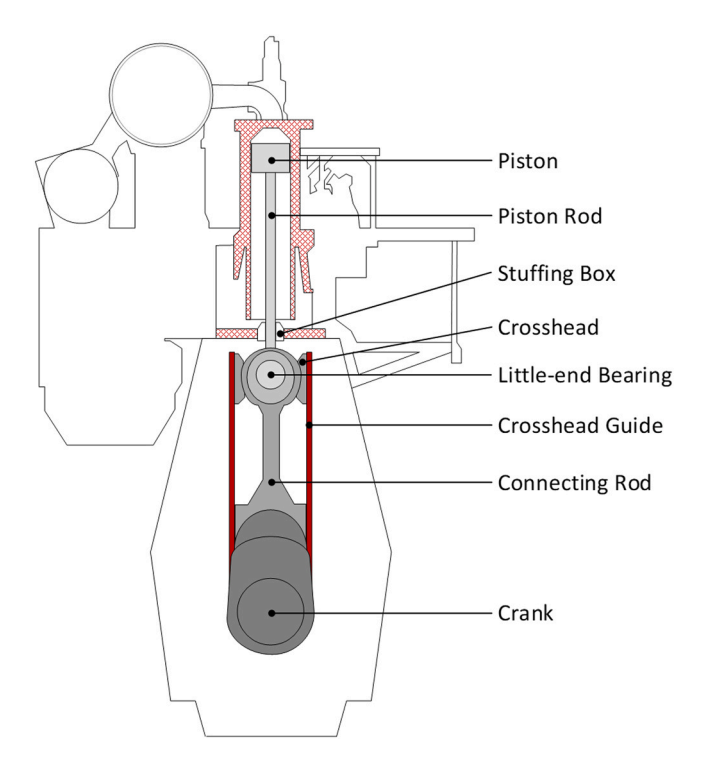


Fig. 1. Schematic design of a large two-stroke marine diesel engine.

supply of lubricant, for both environmental reasons, and to reduce the financial cost of operation. (Approximately 1.18 million tonnes of cylinder lubricant was estimated to be consumed by the world fleet of large two stroke marine vessels annually in 2006 [5] and while typical lubrication rates have fallen over the period since that assessment, this consumption figure remains higher than the level required for lubrication as the flow rate is principally determined by the (higher) lubricant flow rate required to supply additive to neutralise corrosion.)

Traditionally large two-stroke engine cylinders have been lubricated using one or more rows of "quills", small ports in the cylinder which admit oil to lubricate the passing ring pack. This oil was conventionally pumped relatively slowly by a plunger and barrel (Vogel type) arrangement. In more modern designs lubricant is supplied in a pulse of oil in the form of a spray or droplets [6]. The latter approach sometimes makes use of the flow of air into the engine to disperse the oil onto the cylinder ahead of the passing piston more evenly and effectively than is possible with plunger systems. This method also appears to facilitate a reduction in the required oil supply rate [6].

Oil transport mechanisms in lubricated contacts have been studied extensively in engines for road-going vehicles, where lubricant is supplied beneath the piston from the crankcase. Theoretical and experimental studies have mainly focused on the axial transport of lubricant, and it has been shown that a number of mechanisms are probably responsible for the motion of lubricant along the engine cylinder. These include:

- Hydrodynamic transport of excess oil when the inlet is overfilled [7]
- Droplet transport in the two-phase fluid which passes through piston-ring gaps [8]
- Transport by "ring pumping" [9]
- Incidental transfer in "blow-by" gases, especially during ring flutter
  [9]

Experimental measurement of lubricant flow has been attempted in engines. One approach includes sampling various forms of "labelled" lubricant through small holes along the axis of the engine cylinder. The method involves motoring or firing an engine using a conventional lubricant, then switching to the labelled lubricant after a period of time. Measuring the time for the labelled lubricant to reach a specific sampling point on the cylinder allows estimates of the lubricant transport rate. A similar method has also been used to measure lubricant residence times in the ring pack. Labelling the lubricant has been achieved using chemical tracers (dyes) [10] and oils with different levels of degradation [11].

Lubricant flow has also been observed qualitatively and quantitatively using laser-induced fluorescence (LIF). This principle of observation has allowed investigation of such features as:

- Oil movement in ring packs and along the piston skirt [12]
- Oil accumulation on the piston crown and second land [13]
- Fuel accumulation in the oil on the cylinder wall [14]
- Fuel transport and its impact on lubrication conditions [15]

In parallel with fluorescence-based studies, electronic sensors have been developed by the authors of this paper for the investigation of piston-ring lubrication. This has allowed, for example, studies into the effect of load and viscosity on film thickness [16], mapping of film extent across the ring and measurement of ring twist [17]. More recently, these electronic sensors have facilitated a method to infer oil transport rates [18]. This approach has been applied in this paper.

The authors have noted that, in contrast to the comparatively large number of open publications investigating lubricant transport in the piston-assembly of road-going vehicles, including some recent work investigating the time needed for the oil-film to fully develop upon engine start-up [19], there are relatively few papers describing experimental and theoretical studies into lubricant transport in crosshead-based systems. Although there is a great deal of overlap in the analysis of lubrication in these engine types it is important to incorporate the nuances of differences in their design as the lubrication of the piston-rings in these two types of engines differs in several important respects:

- i. In marine engines, the cross-head bearings provide the reaction to lateral forces from the connecting rod as opposed to the piston/cylinder liner. As such there are no combustion forces explicitly directed to a "thrust face" in the cylinder area and the dynamics of the piston and the piston-ring pack are, therefore, not the same. The presence of sides forces is more likely to lead to cyclic asymmetry in lubricating film thickness in road transport engines. (In marine engines film thickness variations have been reported during rough seas where varying side loads may be a contributing factor. [20].
- ii. In marine engines the delivery of oil to the cylinders is in the form of a controlled (often spray) injected volume which varies according to engine load and speed. It is delivered to the ring pack above the piston and interacts with the ring-pack as the piston rises. The majority of the lubricant is lost through evaporation or burning in the combustion process. To control consumption lubricant is not necessarily supplied to the ring pack on every stroke or cycle, and the initial axial and circumferential distribution of the lubricant may be uneven.
- iii. In road transport roughly the same quality of oil is supplied on every stroke as the piston rises irrespective of the operating conditions of the engine. The oil is supplied to the ring-pack below the piston and interacts with the oil control ring, which regulates a relatively even supply distribution to the ring pack during the downstroke. The majority of lubricant is returned to the sump and overall oil losses due to evaporation and combustion are very small.

Since a better understanding of oil transport in this type of engine may facilitate the use of lower quantities of lubricant (with a consequent reduction in pollution by combustion products) this paper presents research which includes measurements and predictions of lubricating film thickness and lubricant flow in axial and circumferential directions

during the motored operation of the piston operating with a single ring. The research is part of an extended programme of study aimed at reducing lubricant consumption in marine engines through the use of intelligent, feedback control of the lubricant supply.

#### 2. Summary of the modelling method

Numerous models for computing piston-ring oil-film thickness and predicting friction, lubricant flow rate, blow-by, etc. have been developed over the years [21–25]. These models have progressively improved

and now incorporate many features such as

- accurate predictions of the pressure distribution in the piston-ring and cylinder liner conjunction through improved starvation and cavitation models [22,23],
- the use of algorithms to satisfy flow-continuity [24],
- the inclusion of a second (circumferential) dimension to overcome the need to assume the system is axis-symmetric (for example, to account for lobed bores, where blow-by can be more prevalent) [24],

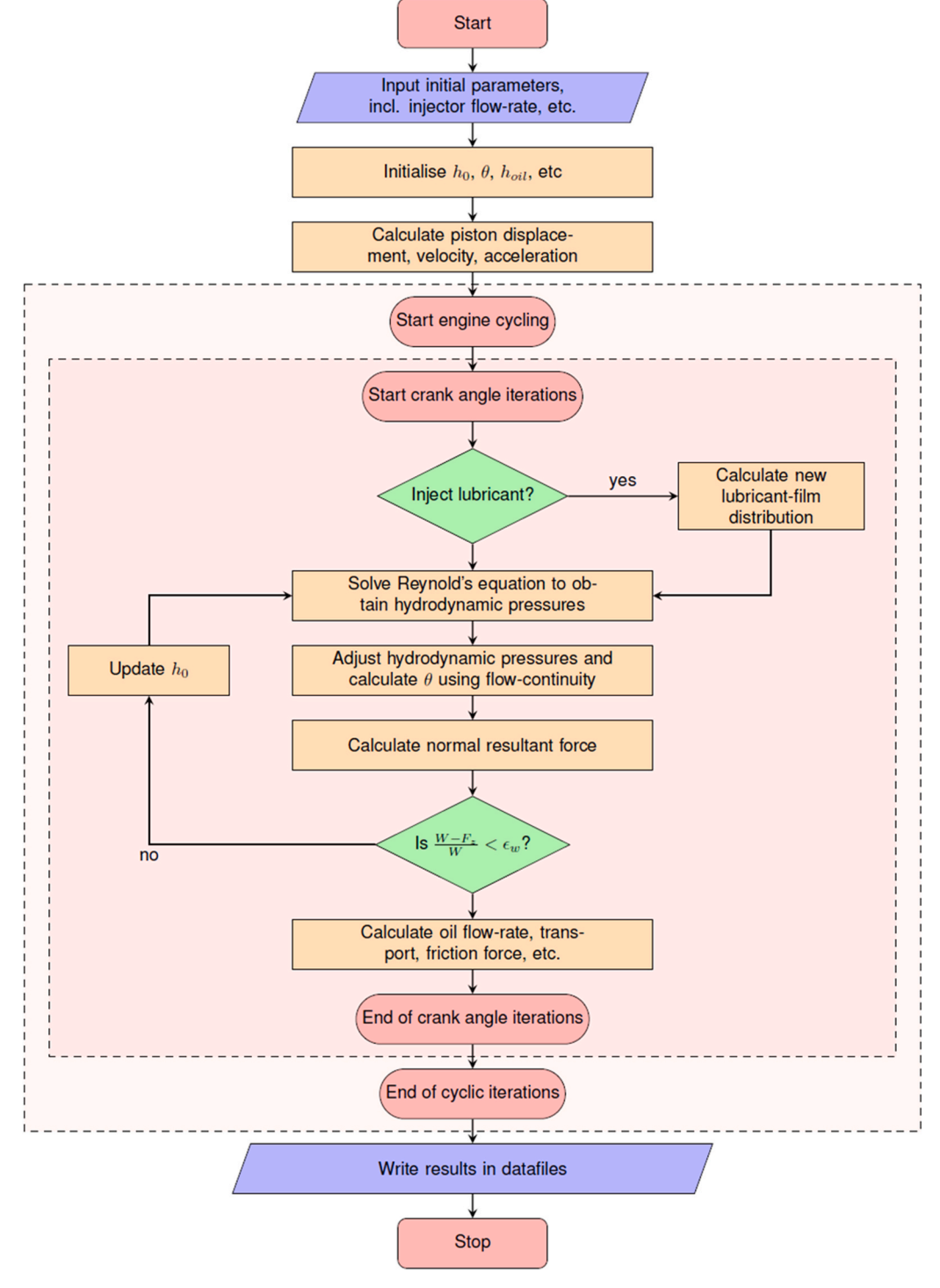


Fig. 2. Computational Flowchart.

• features to describe how lubricant is supplied to the cylinder and transported around it [25].

However, most simulations have been developed for steady-state engine conditions and continue to run only until cyclic convergence is found (ie. when oil-film thickness at a given crank position on the current cycle is within a given tolerance of that on the previous cycle). The algorithm presented in this paper has been developed to predict the lubricating conditions in large marine diesel engines, in which the thickness and distribution of the lubricating film in the cylinder changes from one cycle to the next due to the delivery of lubricant at local positions on the cylinder and at intervals equal to or greater than once every cycle, as illustrated in Fig. 2. As such, the algorithm continues for a pre-determined number of cycles in order to track the development of the oil-film in the cylinder following intermittent and/or non-uniform delivery of oil to the cylinder. This feature allows oil-film thickness, oil transport, the occurrence of blow-by, piston-ring friction and power loss to be predicted over a number of cycles. In addition to its application for large marine diesel engines, the algorithm also has relevance for modelling engine start-up and other transient conditions across a wide range of internal combustion engine types, especially where load and speed varies as in road going vehicles for example.

## 2.1. Flow-continuity algorithm

The algorithm used for computing piston-ring oil-film thickness adopts the flow-continuity method and time-marching procedure described by Ma et al. [26,27]. This procedure is summarised below (and in the flowchart in Fig. 2). The model can evaluate oil-film thickness and frictional losses for cases where the assumption of axis-symmetric conditions does not hold true. For example, with out-of-round cylinder bores, piston-ring eccentricity or, as in this case, where the volume of lubricant supply to the piston-ring varies circumferentially as well as axially. Unlike the scheme described by Ma et al. [26], in this paper lubricant is delivered to the cylinder in a manner to reflect the situation in marine applications where the lubricant is sprayed into the cylinder above the piston and with the initial thickness of the resident oil film varying both axially and circumferentially (Fig. 4). In this instance it is calculated to reflect the distribution from several spray injector nozzles. Injection may occur every cycle, or once every n cycles, when the piston is at bottom dead-centre (where n is the frequency of lubricant delivery). To simplify the challenges, only one compression ring is included in the present first stage model. At each crank angle position the following solution procedure is followed:

- 1. To determine the hydrodynamic pressure at the nth crank angle, an estimate of the inlet boundary using the Couette condition is made, using the lubricant available at the inlet. An approximation of the pressure distribution in the conjunction between piston-ring and cylinder liner is determined by finding the solution to Reynolds equation. This is achieved iteratively using a two-dimensional finite difference scheme, until a convergence criterion is met.
- 2. The solution is refined further using a flow-continuity procedure which enforces conservation of mass to find the true location of inlet and cavitation boundaries as well as the associated pressure distribution. The velocity profile and hence the flow rate of the lubricant is assumed to be defined by the Couette and Poiseuille flow in the axial direction, and the Poiseuille flow in the circumferential direction (since there is no sliding component in this direction). This allows finite difference expressions to be determined for the mass flux terms into and out of each control volume. The squeeze-film effect due to the rate of change of oil-film thickness leads to a further term accounting for the rate of change of mass in the control volume. The flow-continuity procedure adopts a switch function [22] to distinguish between fully filled and partially filled elements, along with a variable for the degree of filling.

- 3. Once the pressure distribution and the position of inlet and cavitation boundaries of the full oil film have been determined, the force due to both the hydrodynamic pressure and gas pressure forces on the piston-ring face are calculated and compared to the sum of the gas pressure force acting behind the piston-ring and the force due to ring tension.
- 4. If the force balance is outside of the required tolerance, the oil-film thickness is updated and the process repeated from step 2, using the previous solution as the initial estimate. If the force balance is within tolerance, the accumulation of lubricant at the leading edge of the piston-ring is computed as the difference between the volume of lubricant available at the inlet and the volumetric flow of oil through the conjunction. This is done at each circumferential control volume. Starvation of the piston-ring inlet implies no accumulation occurs. The volume of lubricant accumulated is transported to and summed with the volume of lubricant available at the next crank angle location. The volume of lubricant at the trailing edge becomes available at this same cylinder location for the following stroke. Friction losses are estimated using a model for boundary or viscous friction, depending on the oil-film thickness and lower-limit for full hydrodynamic lubrication. The algorithm then progresses to the next crank angle position and the process is repeated.
- 5. If lubricant is transported to either top- or bottom-dead-centre, the accumulated lubricant is considered to be consumed. At the present time, no mechanism for lubricant consumption by evaporation is included in the model.

## 2.2. Assumptions and simplifications

- 1. Only one compression ring is modelled, and the piston-ring and cylinder liner are circular and concentric. An operating marine engine generally has more than one piston-ring and it is expected in this case that the rates of hydrodynamic lubricant transport would be greater due to a) additional compression rings repeating the transport action of the first, even if that is to a lesser extent, and b) additional downward motion arising due the influence of the scraper ring.
- 2. Hydrodynamic lubrication is assumed for oil-film thicknesses greater than three times the combined surface roughness (based on the statistical standard deviation of surface heights,  $R_q$ , for the cylinder liner and piston-ring).
- Friction and hence power loss can be evaluated by the model, although this is yet to be validated and not discussed in this paper. Friction forces between the piston-ring groove and piston-ring top and bottom lands are assumed to be negligible for the work presented below.
- 4. The system is considered to be quasi-steady, that is that while some dynamic forces are considered, namely the squeeze-film effect, the algorithm uses static equilibrium of forces at each crank angle position to find the oil-film thickness.

As a first step to validation, the algorithm displayed favourable agreement when compared to Purday's relationship [28] (Eq. 1), for an infinite-width parabolic slider, as illustrated in Fig. 3. Several key parameters of the model are summarised in Table 1.

$$\frac{h_0}{R} = 4.88 \frac{\eta U}{P_y} \tag{1}$$

#### 2.3. Lubricant supply

Large two-stroke marine diesel engines employ several types of systems to deliver lubricant to the cylinder wall. The traditional method is to have several "quills" which supply lubricant to a zig-zag groove on the cylinder liner. An updated version, known as the pulse lubricating system [29], is similar but has improvements to metering and timing.

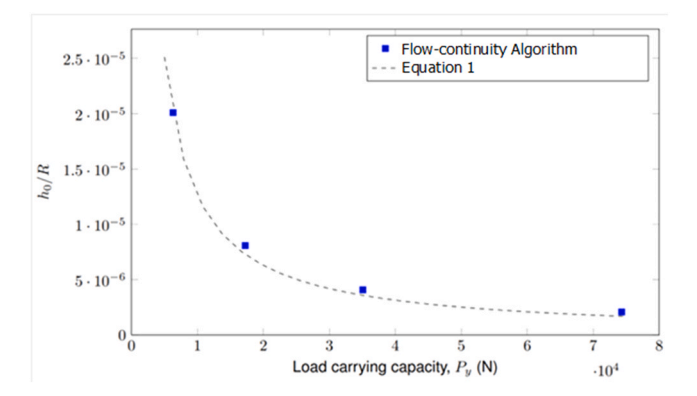


Fig. 3. Comparison of flow-continuity model to Purday's relationship.

**Table 1**Model parameters.

Parameter	Value	Units
Number of axial nodes	48	
Number of circumferential nodes	96	
Equilibrium of hydrodynamic pressure and gas load/ring tension	0.1	%
Flow Continuity Convergence Coefficient for Pressure	$2  imes 10^{-5}$	
Flow Continuity Convergence Coefficient for Degree of Filling Maximum number of iterations for flow continuity	$\begin{array}{c} 1\times10^{-5} \\ 2000 \end{array}$	

The swirl injection principle [30] utilises spray nozzles to inject lubricant into the combustion chamber gas flow, and uses the swirl induced by the piston to improve the spread of lubricant around the cylinder liner. While it would be possible in principle to develop a modelling procedure to describe lubricant availability in the cylinder following an injection event from any of these systems, the modelling work presented in this paper adopts a different approach, discussed below. This allows direct comparison with the experimental investigations presented here.

The experimental apparatus is fully detailed elsewhere [18]. In summary, lubrication is supplied by four precision spray nozzles each with a 25 degree cone angle. Injectors are positioned above the cylinder liner to deliver lubricant to the top half of the cylinder. Injection pressure is set at 1 bar with a delivery duration set to 0.2 s to ensure all lubricant from the metered injector is delivered to the cylinder. As the experiments are conducted with the cylinder head removed, there is no swirl to help spread the lubricant and so lubricant is assumed to be sprayed directly to the cylinder liner. The change in lubricant availability at all positions within the cylinder can be computed once the

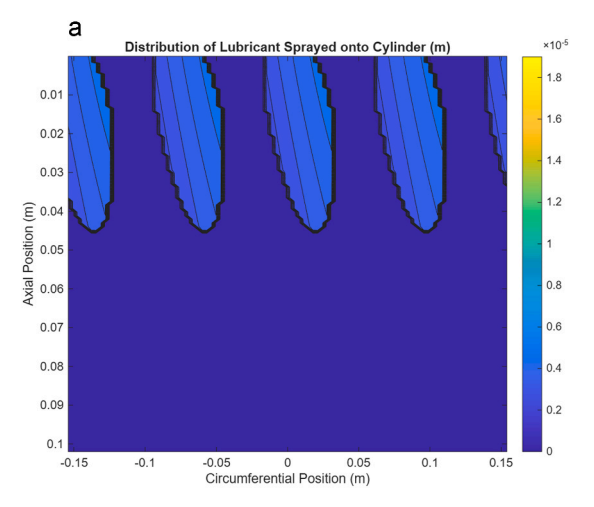
position and orientation of the injector nozzles are specified, along with the spray angle and the volume delivered by each injector on each injection event (which has been validated experimentally). Whilst it is assumed that lubricant is evenly distributed throughout a conical spray pattern, this does not result in a uniform distribution of lubricant on the liner. Fig. 4 shows the distribution of lubricant on the cylinder following a single spray event from the four spray nozzles at high and low flow-rates. A variation in the oil-film thickness across each region of lubricant occurs due to the curvature of the cylinder wall. The procedure for evaluating this distribution is described in detail in appendix A.

#### 3. Model results

The flow-continuity algorithm was therefore executed for a test of 30 s of engine operation at 120 rpm (60 cycles) with two lubricant flow rates; 0.01 millilitres per injection (mL inj<sup>-1</sup>) and 0.04 mL inj<sup>-1</sup>, simulating the operation of a single compression ring. During the design of the experimental equipment, it was calculated that four spray nozzles delivering 0.01 mL of lubricant would lead to a film thickness of 4 µm if the lubricant delivered was spread evenly around the cylinder. Given the expectation that some of this oil would be scraped to top or bottom dead centre, it was deemed to be a suitable starting point for the design and operation of the oil delivery system. Initial experimental tests at the minimum flow-rate of 0.01 millilitres per injection (mL inj<sup>-1</sup>) had shown the oil-film thickness for much of the stroke reached a near steady-state level within 60 cycles. (See Fig. 7 for example). The cylinder pressure was set to ambient conditions in order to correspond to motored engine conditions (with the cylinder head removed). Lubricant was injected on every cycle when the piston was at bottom dead centre. To allow the model to run prior to the first lubricant delivery, an initial nominal oil-film of  $0.8\,\mu m$  was defined at all cylinder locations. Key engine parameters are summarised in table 2. Results data from both the model and experiments is available at https://uclandata.uclan.ac.uk/id /eprint/618

**Table 2**Engine Parameters

Parameter	Value	Units
Bore diameter	98	mm
Crank radius	51	mm
Connecting rod length	165	mm
Axial height of piston-ring	2.8	mm
Radius of curvature of piston-ring face	30	mm
Rotational frequency of engine	120	RPM
Lubricant viscosity	0.155	Pa.s



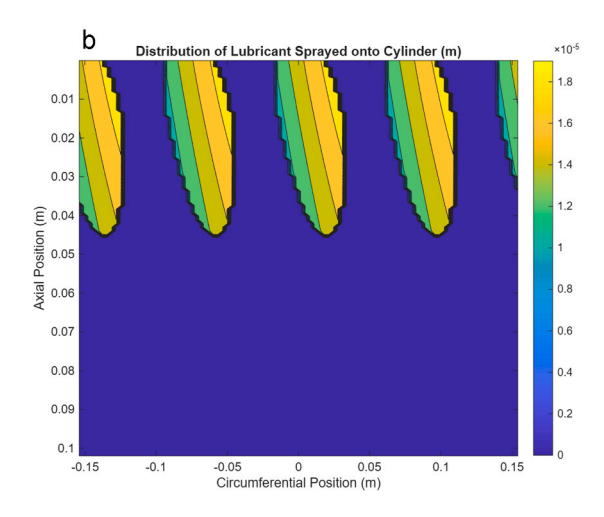


Fig. 4. Computed oil-film thickness on the cylinder from a single injection event.

Fig. 5 shows the predicted oil-film thicknesses develop as the engine cycles at two lubricant flow rates. The results shown are for the 1st, 10th and 20th cycles. On the first cycle, oil-film thickness begins to rise at the same point for both lubricant flow rates, because the area to which lubricant is delivered is the same for both flow rates, even if the volume of lubricant delivered is different. At the higher flow rate the increased volume of lubricant on the cylinder then leads to greater oil-film thickness. The different levels of oil availability in the earlier strokes give rise to differences in film thicknesses between the up and down strokes. After the 10th cycle, the film thickness patterns are virtually identical on both strokes, and there is little difference between the predictions at the two flow rates. This is because adequate lubricant is being supplied to the ring.

#### 4. Comparison of experimental and theoretical data

The experimental apparatus [18] has a highly configurable oil injection system with four injectors which allow the apparatus to be operated using a range of injection supply volumes and injection sequences. The system uses capacitance-based oil film thickness sensors to make estimates of lubricant flow rate which are consistent with theoretical predictions of oil film thickness development and oil flow at start-up. Details of these transducers and their calibration are presented in [31].

#### 4.1. Lubricant distribution

An experiment using this apparatus, emulating the model, was conducted in which the engine was cycled for 30 s at a speed of 120 rpm, ie. a total of 60 cycles. During this time, lubricant was sprayed into the cylinder at four locations on every cycle when the piston reached bottom dead centre (shown in Fig. 6a as positions I, II, III and IV). The experiment was performed with a lubricant flow rate of 0.01 millilitres per injection (mL inj<sup>-1</sup>). Matching the simulation, only the compression ring was employed in these tests. The oil-film thickness was measured by the oil film thickness transducers (shown in Fig. 6b and labelled A-1 to E-8) as the piston-ring passed on every stroke of each test.

#### 4.2. Variation of lubricating film thickness after start-up

Fig. 7 shows the change in minimum oil-film thickness with time for the piston-ring at 4 axial positions in the cylinder (locations 3 through 6, which correspond with crank angles 30, 60, 90 and 120 degrees before/ after top-dead centre). The figure is arranged such that from left to right the change in oil-film thickness is shown at these positions on the upstroke (ie. moving progressively towards top-dead centre), followed by the oil-film thickness measured by the same transducers but on the downstroke. Each individual line shows oil-film thickness against time, for a 30 s period. Experimental results from two circumferential positions are also shown (blocks C and D), along with results from the theoretical model. There are a couple of curious features with these results. At transducer 4, the oil-film thickness at block D is much greater than block C. Anomalous data may be transducer loosening during testing or an issue with one of the replicas taken of the in-situ transducers leading to incorrect measurement of the recess depth (the 'offset') for this. The pre- and post-test replicas of transducers C-4 and D-4 are shown in Table 3. While the difference between the offsets prior to testing was only 1.6 µm, afterwards it was 7.2 µm - which is roughly the difference between the results from each sensor. Although the quality of the scans for these transducers appeared to be good, if one of the had moved, or one of the replicas was compromised (ie. through stretching) this could adversely affect the scans and lead to this discrepancy. Despite this, the overall changes in oil-film thickness through the experiment are in line with each other. At transducer 5 there are some negative oil-film thicknesses measured, which of course is not possible. Since the cylinder was dry when each experiment began, it is possible that the conjunction between the piston-ring and transducer was not completely filled with oil. Since air has a lower relative permittivity than oil, it could lead to negative oil-film thickness once the offset calibration is applied. (This data was not used for the oil transport analysis presented in Section 4.5.)

The model shows the typical variation of minimum oil-film thickness over each stroke, with higher values at mid-stroke than at top and bottom dead centre. The first few cycles are an exception, as lubricant is delivered only near top dead centre and therefore not yet being present in the lower half of the stroke. Results from the experiment show higher

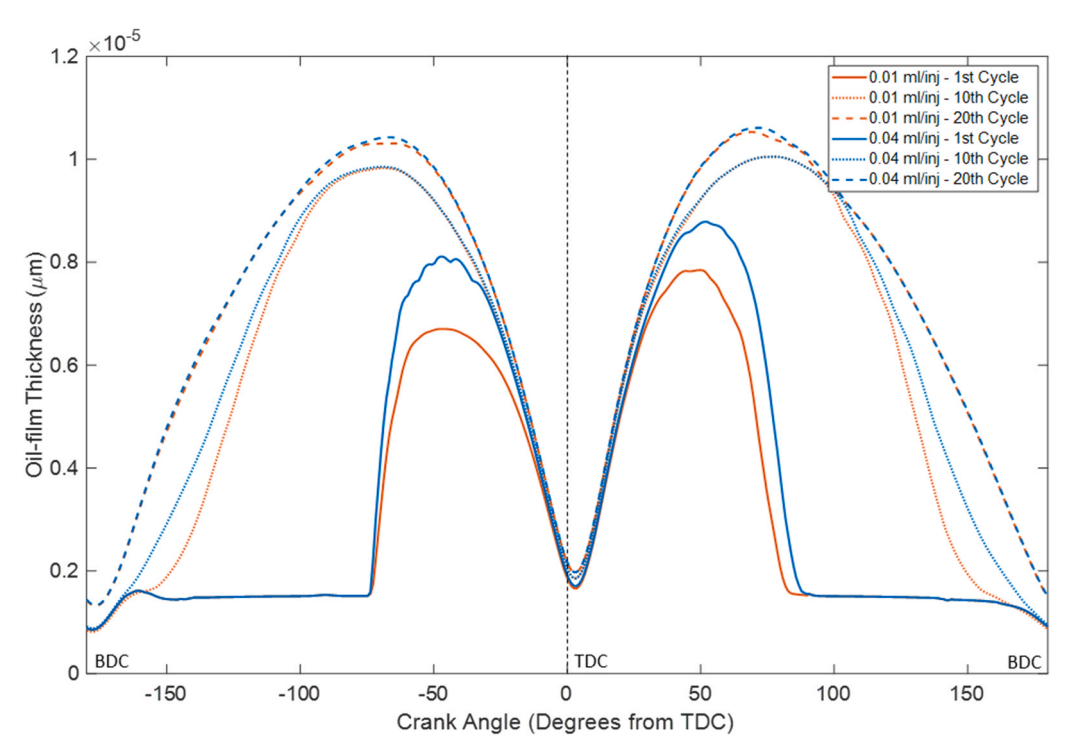
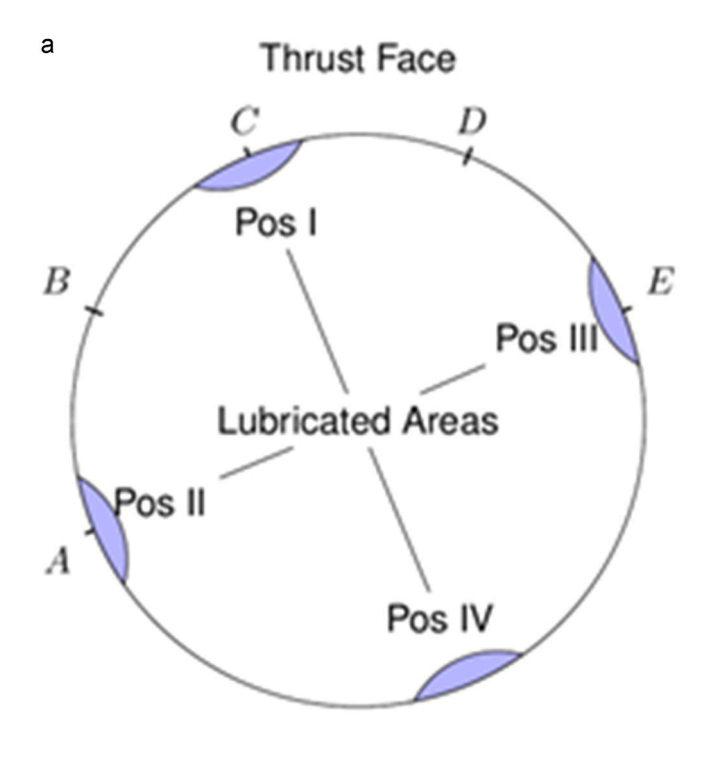
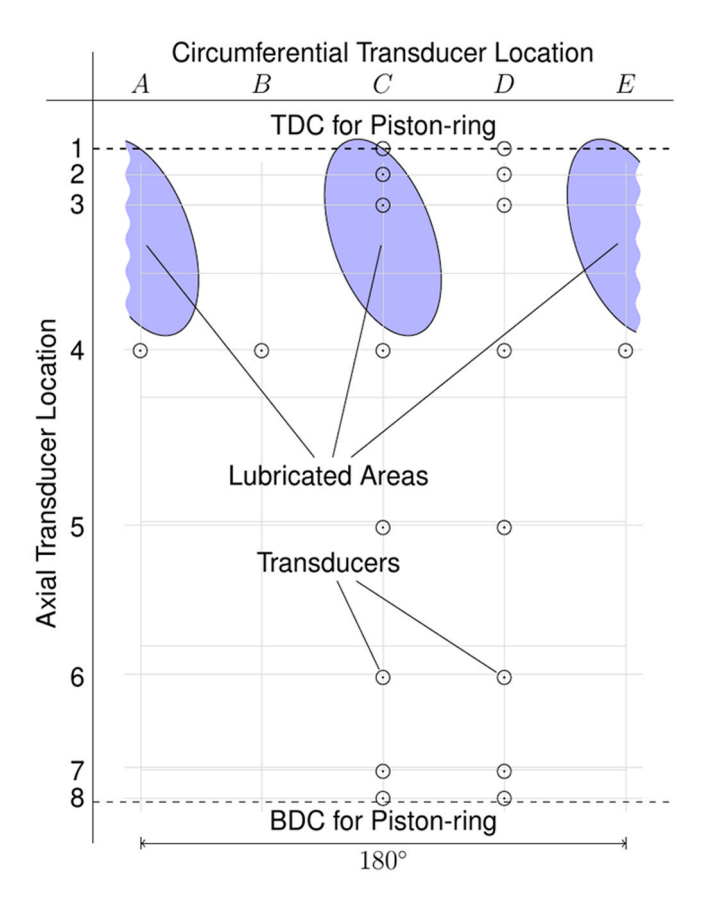


Fig. 5. Predicted Minimum Oil-film Thickness at two lubricant supply rates.



b



**Fig. 6.** Diagram of cylinder showing lubricated areas and transducers. **Fig. 6b** only shows half the circumference – the other half does not have any transducers.

oil-film thickness towards top dead centre, which may suggest the oil does not get transported to mid-stroke and below as quickly as it does in the model. The measurement point 3 in Fig. 6 and Fig. 7 is located in the oil injection area. During the 30-second measurement period, the oil film thickness here varies significantly due to the injected lubricant, although the excess lubricant is scraped away by the piston-ring as it passes.

The model appears to underestimate oil-film thickness near top dead centre, but over-estimates it near to the mid-stroke. The thrust load acting on the piston (which is not included in model) is highest near mid-stroke and may be a factor with this behaviour.

#### 4.3. Changes in degree of filling of filling after start-up

Time-based changes in the degree of filling of the ring/cylinder interface (from inlet to outlet) for the model and the experiment following start-up are shown in Fig. 8(a) to (f). In these figures the piston-ring inlet is on the left, and the outlet on the right. The film extent for the experiment was determined by inspecting the oil-film thickness signals and comparing the measured ring shape to a simulated signal of the true ring profile, as described in [18]. Measured film extent is shown with a solid line and buff shading. The predicted inlet and cavitation boundaries from the model are shown with a dashed line. Each figure also shows minimum oil-film thickness on the right-hand side for reference, again the solid line shows results for the experiment and the dashed lines are results for the model. The vertical axis is time, to show how film extent changes during the test.

Inspecting the data for transducers D3, D4 and D5, the model predicts the piston-ring to be fully starved throughout the test. Lubricant is not delivered to this section of the cylinder in the experiment and needs to be transported circumferentially to it. This does not occur within the time frame of the model, but it is clearly accomplished in practice, perhaps a result of unmodelled effects such as the action the piston face against the cylinder, piston-ring eccentricity and tilt, or inertial spreading. The piston-ring is well supported by lubricant elsewhere and due to the assumption of concentricity the oil-film thickness, is still shown to increase. For the transducers C3, C4 and C5, the film extent for both the model and the experimental results show a transition from starved to fully flooded. At transducer C3 this occurs at the very beginning of the test. Lubricant is delivered directly to this area of the cylinder and so this should be expected. For C4, the predicted results show this transition to occur sooner than seen in the experiment, suggesting the transport of lubricant axially is quicker in the simulation than for the experiment. For transducer C5 the situation is less clear cut. The data show an almost fully flooded ring until 10 s into the test, followed by a period where it is much more starved, and finally a transition back to fully flooded. This may have been caused by a splash of oil from the injector (which eventually gets scraped away) or contact between the piston-ring and cylinder until the time when lubricant is scraped to this area of the cylinder.

#### 4.4. Movement of the cavitation boundary

The time-based changes in the cavitation boundary at the ring to liner interface after start-up appear to be well predicted at transducers C3, C4 and C5.

As would be expected, there is a clear link between the degree of filling and oil-film thickness. This is shown in the results at most of the transducers, both experimental and those from the model. At the same time the cavitation boundary also moves slightly towards the trailing edge of the piston-ring. Also, oil-film thickness can be seen to increase at times when there is no change to the degree of filling (either when starved or fully flooded). This must therefore be due to the transport of lubricant in the circumferential direction. This appears to occur more slowly than the rate at which the piston-ring fills in the axial direction, which the results show to take just a few cycles.

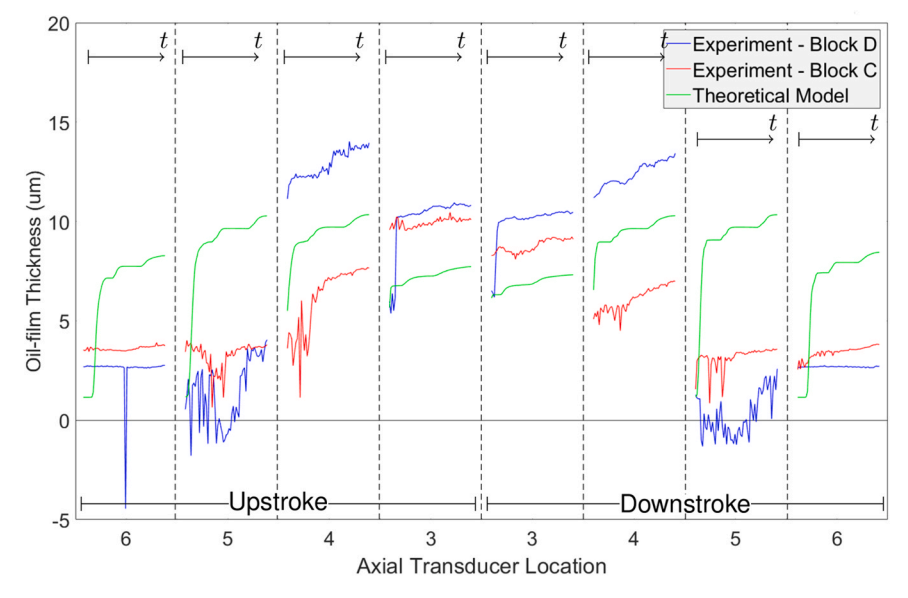


Fig. 7. Oil-film thickness vs. Time at different locations in the cylinder (upstroke and downstroke).

**Table 3**Pre- and post-experiment offsets for transducers C-4 and D-4.

	Transducer C-4	Transducer D-4
Pre-test	1.1 μm	2.7 μm
Post-test	-2.2 μm	5.0 μm

#### 4.5. Linkage between oil-film thickness and degree of filling

Fig. 9 shows the variation of minimum oil-film thickness at two of the transducers following start-up. Data for the upstroke (solid) and downstroke (dashed) are shown for both the experiment (orange) and from the model (blue). The film thickness data from the model and the experiment appear to correlate reasonably well. There is some error in the absolute magnitude. However, the rate at which oil-film thickness increases is well captured by the model.

It is evident from the theoretical data that the oil film increases in several distinct 'stages', suggesting there are underlying time constants behind the development of the oil film in the cylinder. These 'stages' can also be seen in the experimental results. The authors believe various time constants relating to each stage correspond to the method by which the cylinder is lubricated and the manner in which the conjunction between the piston-ring and cylinder fills with lubricant.

STAGE 1 (1–10 cycles): The first stage is a relatively rapid increase corresponding to the transition from a starved to a fully flooded inlet, at least at some of the circumferential positions. At the location of transducer C-3, this occurs after the first cycle since it is at a position where lubricant is sprayed onto the cylinder. At the C-4 transducer location filling is somewhat more gradual as it requires lubricant to be transported downwards to this location. For the experimental data there is a longer delay before the oil-film thickness begins to increase. The authors suggest the first time-lag may correspond to the rate at which the pistonring inlet is filled.

STAGE 2 (15–25 cycles): The mechanism of the second stage is perhaps less apparent. It is thought this might be due to the filling and subsequent increase in oil-film thickness at other axial locations in the cylinder. If, on an upstroke say, the oil-film thickness is higher, then even if lubricant availability nearer to TDC is the same as the previous cycle the oil-film thicknesses here will be greater due to the reduced squeeze effect.

STAGE 3: (>20 cycles)The third 'stage' in film development appears to relate to the widening of the fully flooded region between piston-ring

and cylinder. Fig. 10 shows the conjunction between the piston-ring and cylinder liner. The horizontal axis represents the circumference of the piston-ring face and the vertical axis the piston-ring width. Fully filled regions are shown in magenta, whereas other shades show the conjunction is only partially filled. The figures show the conjunction continues to be filled circumferentially throughout the simulation, albeit at a slower rate than occurred in the experiment for the reasons outlined in Section 4.2. Since the piston-ring in the model is not flexible and is concentric with the cylinder this will lead to an overall oil-film thickness increase at all circumferential locations. In the experiment the piston ring is not necessarily concentric to the cylinder, which may be why this effect is not as noticeable in those results.

## 4.6. Oil transport in the cylinder

In [18] the authors showed that net axial cylinder lubricant flow rates could be inferred using oil film thickness measurements. Fig. 11 shows experimental data compared to simulation data from the theoretical model. It is possible to evaluate oil transport with much better resolution using the model, since oil-film thickness is known at one-degree crank angle intervals. However, for the sake of comparison, the predicted results shown here have been evaluated using the same time interval as the experimental results. The solid and dashed lines show the net lubricant transport for the model and experimental results, this being the difference between upstroke and downstroke flow. A positive value indicates net flow in the upwards direction. The predicted results show that up until the 15th cycle, there is a greater flow rate on the downstroke than the upstroke. From the 15th cycle onwards there is a higher flow rate on the upstroke. The experimental results have a positive peak after 5 cycles, a dip down to net downwards flow at 15 cycles, and then a subsequent increase again until the upwards flow settles to a consistent level after approximately 30 cycles.

The net lubricant flow rate estimated in the experiment is generally two or three times greater than for the model. The experimental data shown in Fig. 11 is based only on transducers in line with the sprayed lubricant (circumferential position C), for which there is a notable difference between upstroke and downstroke oil-film thickness, particularly at transducers 3 and 4. The only variable used to determine lubricant flow is the difference in oil-film thickness on the down and up strokes and this factor limits the applicability of this approach to flow rate estimates. There are several reasons for this, including the influence of squeeze on film thickness and the assumption of symmetry in the

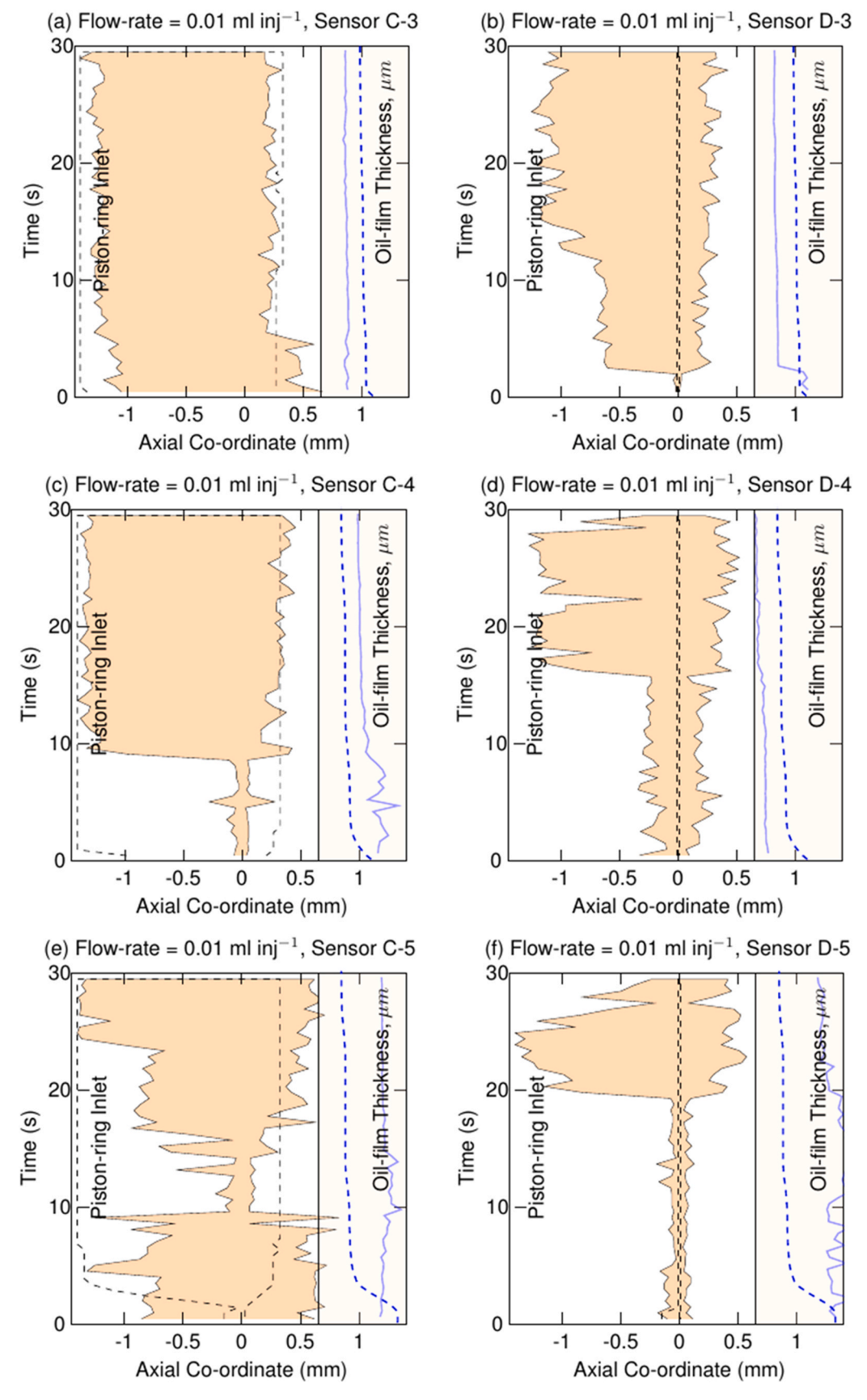
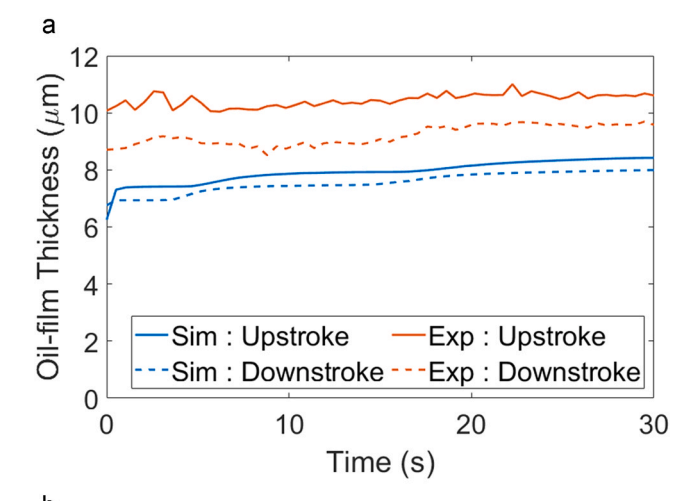
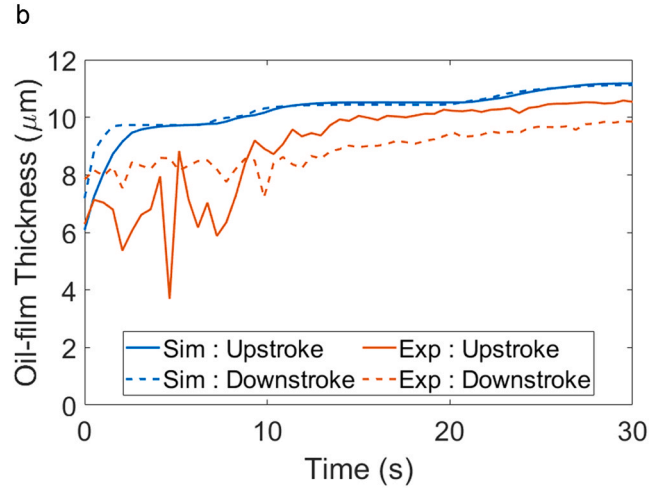


Fig. 8. Film extent at different locations in the cylinder (upstroke).





**Fig. 9.** Minimum oil-film thickness at transducers C-3 and C-4, Model vs. Experiment for upstroke and downstroke.

simulation which will not be reflected in the experimental ring to cylinder interface.

Influence of interface asymmetry: The model assumes the piston-ring is circular and concentric with the cylinder liner and so oil-film thickness is influenced by lubricant supply all around its circumference. Hence the predicted results are influenced also by the lower lubricant supply at other circumferential locations, whereas in the experiment the piston-ring is to some extent flexible, and free to move radially and so the impact of less well lubricated areas on the oil-film thickness at well lubricated areas is likely to be less. It is possible this lessens the differences between the upstroke and downstroke oil-film thicknesses used in the calculations for predicted lubricant flow.

Overall trends: The observed trend for both experimental and model data is for a net lubricant flow upwards initially, followed by a reduction in flow rate. The cylinder liner is dry when the experiment commences, or in the case of the model has only a nominal film-thickness. Consequently, the data is dominated by the introduction of oil into the upper part of the cylinder which leads to a much greater oil-film thickness on an upstroke compared to the previous downstroke. After a few cycles (i. e., 15 in the experiment or around 5 for the model) the oil begins to reach the transducers in the lower part of the cylinder and the oil-film thickness here rises rapidly. (This is also evident in the results of Fig. 8). Additionally, the upper part of the cylinder is now well lubricated and so the operating film thickness has settled and the difference in oil-film thickness from one cycle to the next is small in comparison. As a result, the downwards flow of oil dominates the result. After this phase there is a gradual increase in upwards flow again since much of the

lubricant sprayed onto the cylinder on each cycle is simply scraped upwards to top-dead centre. There is still some transport of lubricant in the downwards direction, but it is outweighed by upwards transport in the top third of the cylinder.

#### 5. Conclusions

This paper describes an investigation of spray lubrication in a reciprocating engine simulator to study oil transport effects. It has demonstrated

- Axial and circumferential spreading occurs at different rates and is driven by physically different processes. Axial flow of lubricant occurs by the scraping action of the ring as the inlet fills. Hydrodynamic pressure in the contact causes lubricant to spread circumferentially, but less quickly than in the axial direction.
- The process of filling and circumferential lubricant spread takes place in a stepwise fashion.
- As the degree of inlet filling increases there is greater circumferential flow
- Close to the lubricant deposition area, typically less than 15 engine strokes are required for the degree of filling to reach 90 % of its final value. Whereas, 50–60 strokes are required for the circumferential spread of lubricant to increase to around 90 % of its steady state level.

This research is part of an effort to address reductions in the lubricant consumption in marine engines through the use of intelligent, feedbackcontrol of the lubricant supply. This approach, described in [32] provides a means of reducing the cost of marine engine lubrication as well as reducing the harmful emissions derived from cylinder lubricant combustion. In this context some important steps forward have been made in understanding how such a system could be realised. While it is possible to use the oil-film thickness sensors alone to react to changes in oil-film thickness with the injection of lubricant, understanding the rate at which the oil-film develops in the cylinder allows a more sophisticated and pro-active control algorithm to be developed. Such knowledge gives predictive capability to facilitate further reducing lubricant consumption while still ensuring the piston-rings are hydrodynamically lubricated. The understanding gained regarding oil-transport circumferentially around the cylinder suggests there is value to be gained in improving any initial distribution of oil around the full circumference of the cylinder. This also simplifies any control system design somewhat, since the injection and axial transport of lubricant at each circumferential position from one injector to the next is largely independent of its neighbour. Better initial distribution will help where sea conditions or wear leads to different lubrication states around the cylinder.

The paper has described a novel experimental study as well as a multi-cycle, simulation model which predicts axial and circumferential flow rates on an instantaneous basis. The model has been developed to accommodate a range of lubrication scenarios for the specific spray pattern of the experimental apparatus employed. For other engine designs, if the distribution of lubricant from the oil delivery system is known, or if the specifications of the spray nozzles can be measured or modelled, then other lubricant application mechanisms and spray patterns can be incorporated into the simulation.

The results have demonstrated that it is feasible to make reliable models to predict oil flow in the absence of the combustion processes that are normally present in internal combustion engines. The study represents a first step towards developing an approach to predict the amount of lubricant that should be injected into a two-stroke engine to maintain adequate lubrication. However, to make this model more realistic will require both the modelling of a more complete ring-pack and the inclusion of a lubricant consumption mechanism based on combustion/evaporation processes.

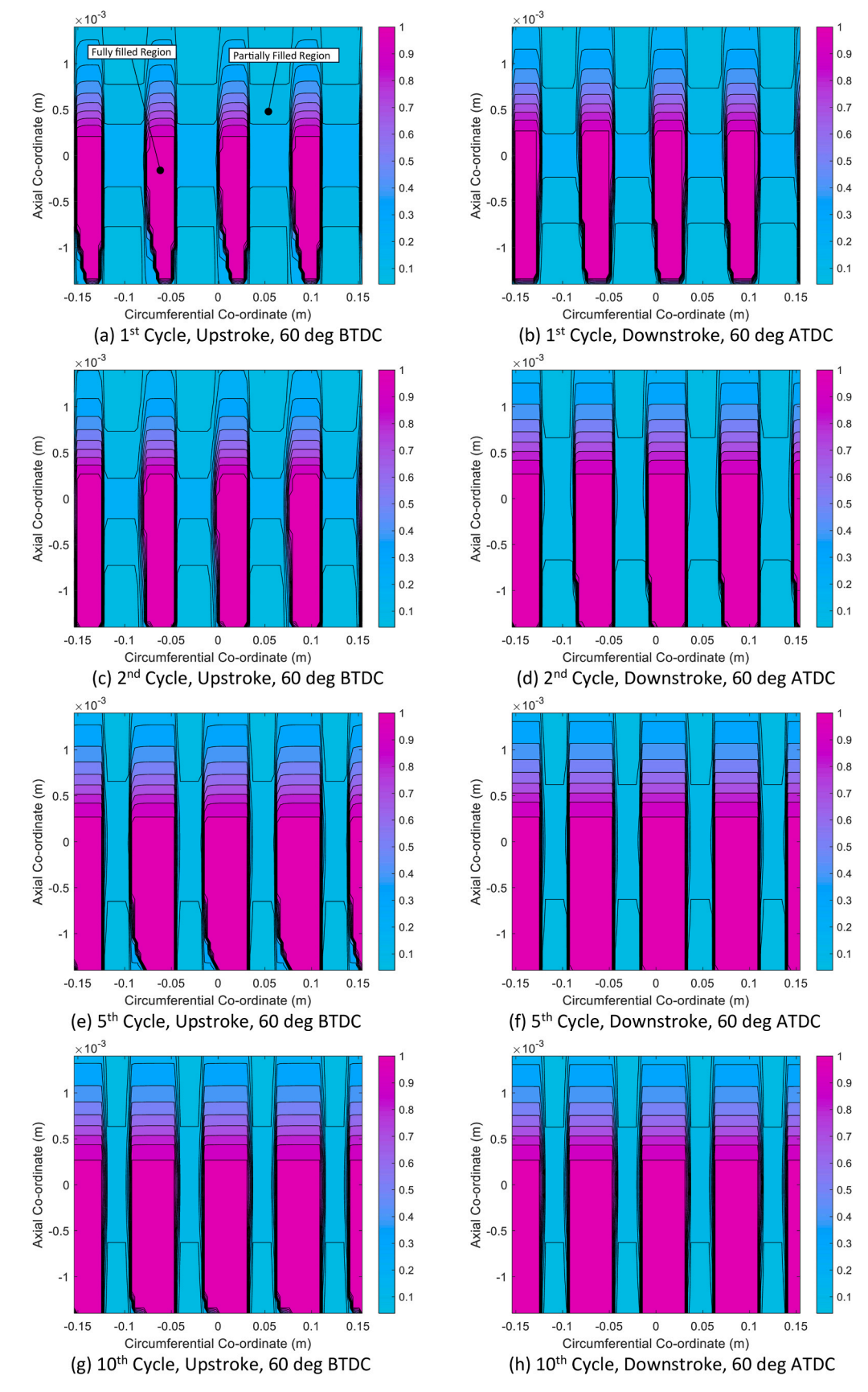


Fig. 10. Predicted degree of filling at axial position of transducer C/D-4.

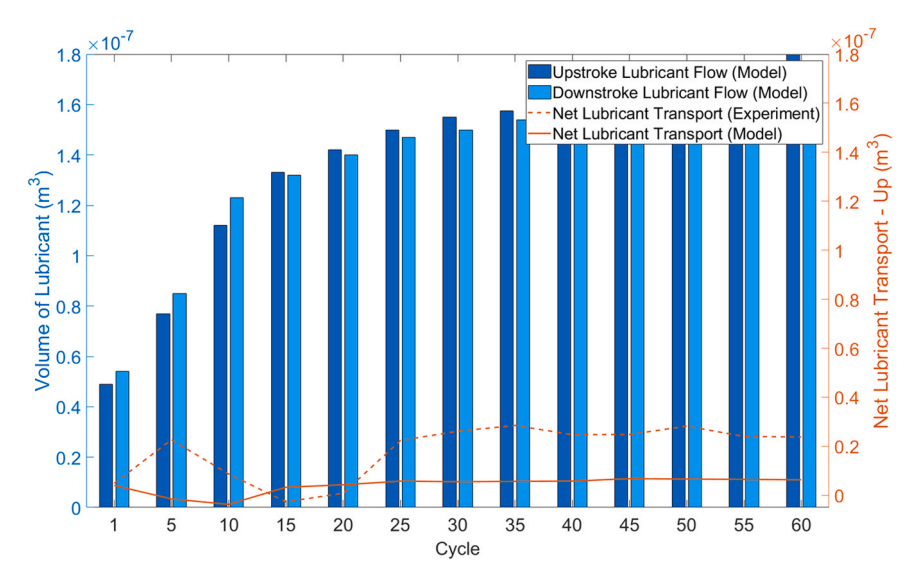


Fig. 11. Axial lubricant flow/transport as determined by experiment and from the model.

#### Statement of originality

As corresponding author, I Graham Calderbank, hereby confirm on behalf of all authors that:

- The manuscript has not been published previously, that it is not under consideration for publication elsewhere, and that if accepted it will not be published elsewhere in the same form, in English or in any other language, without the written consent of the publisher.
- 2. The manuscript does not contain material which has been published previously, by the current authors or by others, of which the source is not explicitly cited in the manuscript.

## CRediT authorship contribution statement

G Calderbank: conceptualization, methodology, software, validation, formal analysis, investigation, writing - original draft. I

**Sherrington:** conceptualization, formal analysis, writing - original draft and review and editing, supervision. **EH Smith:** formal analysis, writing - review and editing, supervision.

#### **Declaration of Competing Interest**

The authors declare the following financial interests/personal relationships which may be considered as potential competing interests: Ian Sherrington has patent #PCT/GB2000/004920 issued to University of Central Lancashire. If there are other authors, they declare that they have no known competing financial interests or personal relationships that could have appeared to influence the work reported in this paper.

#### Acknowledgements

This work was supported by the University of Central Lancashire.

### Appendix A

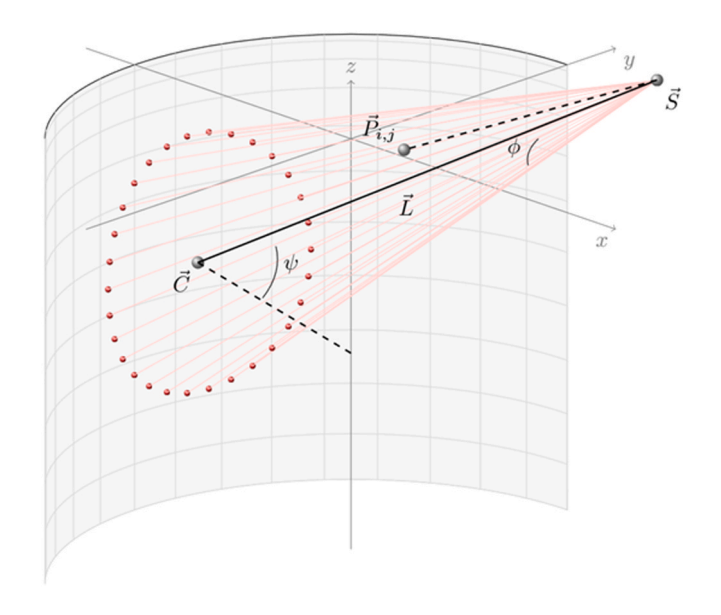


Figure A1.

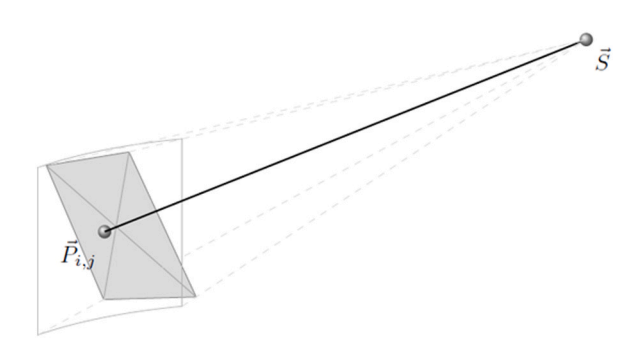


Figure A2.

1. The swept face of the cylinder liner is divided into a grid of  $n_{CA} \times n_y$  nodes for consistency with crank angle stepping and the grid defined for the piston-ring in the circumferential direction. The position  $\overrightarrow{P}$  (in Cartesian coordinates) of each node is determined from the nominal bore diameter and stroke length. The position  $\overrightarrow{S}$  and orientation  $\overrightarrow{L}$  of each injector is also known allowing the intersect to be found between a line (representing the centreline of the cone of lubricant spray) from the injector and the cylinder liner  $(\overrightarrow{C})$ . The line connecting the injector and intersection can be expressed by the vector

$$\overrightarrow{L} = \overrightarrow{C} - \overrightarrow{S}$$
 (A1)

- 2. The angle  $(\phi)$  subtended between the vector from each node to the injection point  $(\overrightarrow{P} \overrightarrow{S})$ , and the vector  $\overrightarrow{L}$  is assessed to determine if it is within the limits of the cone of lubricant spray from the injector (Fig. A1). The injectors have been specified to have a cone angle of 25°, and thus lubricant will be delivered only to nodes where the angle between vectors is below 12.5°.
- 3. While the lubricant spray is assumed to be distributed equally throughout the cone, the volume of lubricant received at each node will not be equal due to the varying incidence angle of the cylinder at each node relative to the injection point. The area of each grid element  $(A_p)$  on the liner can be calculated with Eq. A2. The normal to each cell intersects the axis of the cylinder liner (x = 0, y = 0), and this normal  $(\vec{n}_p)$  is given by Eq. A3.

$$A_p = \frac{d}{2}d\theta dz \tag{A2}$$

$$\overrightarrow{\boldsymbol{n}}_{p} = \begin{bmatrix} \boldsymbol{x}_{p} & \boldsymbol{y}_{p} & 0 \end{bmatrix} \tag{A3}$$

The angle between the vector  $\vec{L}$  and the normal to each cell area can be computed using Eq. A4, in order to find the projected area in the direction of the lubricant injector found using Eq. A5 (Fig. A2).

$$\psi = \frac{\cos^{-1}\left(\left[\overrightarrow{P} - \overrightarrow{S}\right] \cdot \overrightarrow{n}_{p}\right)}{\left[\overrightarrow{P} - \overrightarrow{S}\right] \cdot \overrightarrow{n}_{p}} \tag{A4}$$

$$A_{ps} = A_p \cos \psi$$
 (A5)

4. The total volume of lubricant delivered is shared between the incident nodes based on their proportional areas facing the injection point. The process above is repeated about the cylinder axis every 90 degrees. Where there are overlapping sections the volumes are summed. The change in oil-film thickness at each node is found by dividing the delivered volume to the node by the area Ap. This is added to any residual oil-film already present on the cylinder liner.

## Data availability

I have shared the link to my data in the manuscript

### References

- [1] Penner, J.E., Lister, D.H., Griggs, D.J., Dokken, D.J., and McFarland, M. Aviation and the Global Atmosphere: A special report of IPCC Working Groups I and III. 1999 (http://repository.upenn.edu/cgi/viewcontent.cgi?article=1066&context=library\_papers).
- [2] Endresen E, Sørgård JK, Sundet SB, Dalsøren IS, Isaksen TF, Berglen GGravir. Emission from international sea transportation and environmental impact. J Geophys Res Atmospheres 2003;108:1984–2012.
- [3] Vianaa M, Hamming P, Colettec A, Querola X, Degraeuwed B, De Vliegard I, et al. Impact of maritime transport emissions on coastal air quality in Europe. Atmos Environ June 2014;90:96–105.
- [4] Atkinson D. Onboard condition monitoring of cold corrosion in two stroke marine diesel engines. Int J Cond Monit August, 2015;5(2):17–22.
- [5] Sherrington, I., Shorten, D. Influences on the Lubrication of Piston-Rings in Large Two Stroke diesel Engines and the Impact of MARPOL VI. Proc LUBMAT 2006 pp 185- 189.
- [6] Anonymous Two stroke main engine cylinder lubrication explained. Chief engineers Log (2nd May 2022) (https://chiefengineerlog.com/2022/05/02/two-stroke-main-engine-cylinder-lubrication-explained/).
- [7] Ma M-T, Sherrington I, Smith EH. Implementation of an algorithm to model the starved lubrication of a piston-ring in distorted bores; prediction of oil flow and onset of gas blow-by Proc I Mech E (Part J) 1996;210:29–44 (Journal of Engineering Tribology).

- [8] Gamble RJ, Priest M, Taylor CM. Detailed analysis of oil transport in the piston assembly of a gasoline engine. Trib Lett February 2003;14(2):147–56.
- [9] Thirouard, B., and Tian, T. Oil transport in the piston-ring pack (Part 1): Identification and characterisation of the maim oil transport routes and mechanisms, JSAE Paper 20030345 / DAE paper 2003-01-1952.
- [10] Notay, R.S. Evolution of Lubricant Degradation and Lubricant behaviour in Piston Assembly of a Reciprocating Diesel Engine. PhD Thesis University of Leeds (2013).
- [11] Stark M, Gamble R, Hammond C, et al. Measurement of lubricant flow in a gasoline engine. Tribol Lett 2005;19:163–8. https://doi.org/10.1007/s11249-005-5096-1.
- [12] Sanda S, Konomi T. Development of a scanning laser induced fluorescence method for analysing piston oil film behaviour. IMechE Pap 1993;465/014.
- [13] Thiouard, B.P., Tian, T. and Hart, D.P. Investigation of oil transport mechanisms in the piston ring pack of a single cylinder engine, using two-dimensional laser fluorescence. SAE Paper 982658.
- [14] Parks JE, Barber TE, Storey JME, Wachter EA. In situ measurement of fuel in the cylinder wall film of a combustion engine by LIF spectroscopy. Appl Spectrosc 1998;52:112–8
- [15] Mueller T, Wigger S, Fuesser H, Kaiser S. Development of a LIF-Imaging system for simultaneous High-Speed visualization of liquid fuel and oil films in an optically accessible DISI engine. 2018-01-0634 SAE Tech Pap 2018. https://doi.org/ 10.4271/2018-01-0634
- [16] Söchting SJGH, Sherrington I. The effect of load and viscosity on the minimum operating oil film thickness of Piston-Rings in internal combustion engines. Proc IMechE Part J (Eng Tribology 2009;223(J3):383–91.
- [17] Garcia Atance Fatjo G, Smith EH, Sherrington I. Mapping lubricating film thickness, film extent and ring twist for the compression-ring in a firing internal combustion engine. Tribology Int Oct., 2013;70:112–8.
- [18] Calderbank GJ, Smith EH, Sherrington I. Experimental measurement of the time-based development of oil film thickness, lubricating film extent and lubricant transport rate in cross-head engines. Lubricants Dec., 2020;9(1). https://doi.org/10.3390/lubricants9010004
- [19] Rooke J, Brunskill H, Li X, Taghizadeh S, Hunter A, He S, et al. Piston ring oil film thickness measurements in a four-stroke diesel engine during steady-state, start-up and shut-down. Int J Engine Res 2022;24(4):1499–514. https://doi.org/10.1177/ 14680874221088547

- [20] Moore, S. The complexities of piston ring lubrication in large two stroke marine diesel engine. Proc. CIMAC Congress (Copenhagen, 1988), pp 575 – 586.
- [21] Furuhama S, Sumi T. A dynamic theory of Piston-Ring lubrication. Bull JSME 1960; 4(16):744–52.
- [22] Elrod, H.G. and Adams, M.L., A Computer Program for Cavitation and Starvation Problems, Leeds-Lyon Conference on Cavitation, Leeds University. pp. 37–41 (1974).
- [23] Vijayaraghavan D, Keith Jr TG. Development and evaluation of a cavitation algorithm. Trib Trans 1989;32(2):225–33.
- [24] Ma M-T, Sherrington I, Smith E. Implementation of an algorithm to model the starved lubrication of a Piston-ring in distorted bores: prediction of Oil-flow and onset of gas Blow-by Proc Inst Mech Eng Part JJ Eng Tribology 1996;210:29–44.
- [25] Overgaard H, Klit P, Vølund A. Lubricant transport across the piston ring with flat and triangular lubrication injection profiles on the liner in large two-stroke marine diesel engines. Proc Inst Mech Eng Part J J Eng Tribology 2018;232(4):380–90. https://doi.org/10.1177/1350650117715151.
- [26] Ma M-T, Smith EH, Sherrington I. A three-dimensional analysis of piston-ring lubrication. Part 1: modelling. Proc I Mech E (Part J) J Eng Tribology 1995;209: 1–14.
- [27] Ma M-T, Smith EH, Sherrington I. A three-dimensional analysis of piston-ring lubrication. Part 2: sensitivity analysis. Proc I Mech E (Part J) J Eng Tribology 1995;209:15–27.
- [28] Dowson D, Higginson GR. Elasto-hydrodynamic lubrication. International series on materials science and technology. Pergamon Press; 1977. ISBN: 9780080213026.
- [29] Christensen O. Cylinder lubrication of two-stroke crosshead marine diesel engines. Wartsila Tech J 2010.
- [30] Eriksen L. Developments in cylinder liner lubrication. Information Conference. Institut fur Schiffsbetriebsforschung; 2003.
- [31] Calderbank, G., The Effect of Oil Supply on Piston-ring Lubrication in an Internal Combustion Engine. PhD Thesis pp, 94-103. (https://clok.uclan.ac.uk/id/eprint /56900/).
- [32] Sherrington, I., Calderbank, G., Smith, E.H. A New Approach to Cylinder Lubrication in Large Two Stroke Marine Engines. Proc. Of the 20th International Colloquium Tribology Industrial and Automotive Lubrication 12–14 January 2016 Stuttgart / Ostfildern, Germany.